

Supporting information for:

# Hybrid Iron Oxide-Copolymer Micelles and Vesicles as Contrast Agents for MRI: Impact of the Nanostructure on the Relaxometric Properties

Paolo Arosio<sup>‡a</sup>, Julie Thévenot<sup>‡b,c</sup>, Tomas Orlando<sup>‡d</sup>, Francesco Orsini<sup>a</sup>, Maurizio Corti<sup>d</sup>, Manuel Mariani<sup>e</sup>, Lorenzo Bordonali<sup>d</sup>, Claudia Innocenti<sup>f</sup>, Claudio Sangregorio<sup>f,g</sup>, Hugo Oliveira<sup>b,c</sup>, Sébastien Lecommandoux<sup>\*b,c</sup>, Alessandro Lascialfari<sup>\*a,d,h</sup> and Olivier Sandre<sup>\*b,c</sup>

<sup>a</sup> Dipartimento di Fisica, Università degli Studi di Milano, I-20133 Milano, and Consorzio INSTM, ITALY

<sup>b</sup> Université de Bordeaux/IPB, ENSCBP, 16 avenue Pey Berland, 33607 Pessac Cedex, France

<sup>c</sup> CNRS, Laboratoire de Chimie des Polymères Organiques (UMR5629), Pessac, France. Fax: +33 5-4000-8487; Tel: +33 5-4000-3695; E-mail: lecommandoux@enscbp.fr and olivier.sandre@ipb.fr

<sup>d</sup> CNISM, Consorzio INSTM and Università degli Studi di Pavia, Dipartimento di Fisica A. Volta, I-27100, Pavia, ITALY. Tel: +39 03-8298-7499; E-mail: alessandro.lascialfari@unipv.it

<sup>e</sup> Dipartimento di Fisica e Astronomia, Università di Bologna, I-40127, Bologna, ITALY

<sup>f</sup> Dipartimento di Chimica, Università di Firenze and Consorzio INSTM, Sesto Fiorentino, ITALY

<sup>g</sup> ISTM – CNR, I-20133 Milano, ITALY

<sup>h</sup> Istituto nanoscienze – CNR, Modena, ITALY

<sup>‡</sup> These authors contributed equally to this work.

\* Corresponding Authors

<sup>†</sup> Electronic Supplementary Information (ESI): SI-1. Synthesis of iron oxide superparamagnetic nanoparticles, SI-2 Size sorting process of the iron oxide superparamagnetic nanoparticles, SI-3. Characterization of the iron oxide nanoparticles dispersions, Magnetization curves, Selected area electron diffraction. Iron oxide concentration determination. Longitudinal and transverse NMRD profiles for magnetic micelles. Field Cooled (FC) and Zero Field Cooled (ZFC) magnetization curves.

DOI: 10.1039/C3TB00429E

### *SI-1. Synthesis of iron oxide superparamagnetic nanoparticles*

Superparamagnetic nanoparticles made of maghemite ( $\gamma\text{-Fe}_2\text{O}_3$ ) were synthesized in water according to Massart's procedure.<sup>1</sup> At first, magnetite  $\text{Fe}_3\text{O}_4$  nanocrystals (also called ferrous ferrite  $\text{FeO}\cdot\text{Fe}_2\text{O}_3$ ) were prepared from an alkaline coprecipitation of a quasi-stoichiometric mixture of iron +II (0.9 mol) and iron +III (1.5 mol) chloride salts in HCl solution (3 L,  $\text{pH}\approx 0.4$ ). One litre of a concentrated ammonia solution (7 mol) was quickly added onto the acidic iron salts mixture, which produced a black solid suspension almost instantaneously. After 30 minutes of stirring at 800 rpm, the  $\text{Fe}_3\text{O}_4$  nanoparticles were attracted by a strong ferrite magnet ( $152\times 101\times 25.4\text{ mm}^3$ , Calamit Magneti, Milano-Barcelona-Paris). Then the supernatant ( $\approx 2.25\text{ L}$ ) containing non magnetic ferrihydrites (reddish flakes) was discarded and the magnetic precipitate (black) was washed with 1 L of water. After sedimentation on the ferrite magnet, the flocculate was acidified with 0.26 L of nitric acid (69%) and stirred 30 min after being completed up to 2 L with water. In order to completely oxidize magnetite into maghemite, the solid phase was separated from the supernatant ( $\approx 1.5\text{ L}$ , red) and immersed in a boiling solution of ferric nitrate (0.8 mol in 0.8 L). After 30 min under stirring at 90-100°C, the suspension turned into the red colour characteristic of maghemite  $\gamma\text{-Fe}_2\text{O}_3$ . Finally, free ions in excess were removed by washing with acetone and diethyl-ether and the nanoparticles were readily dispersed in water to form a true "ionic ferrofluid" made of maghemite nanoparticles.

### *SI-2 Size sorting process of the iron oxide superparamagnetic nanoparticles*

After the synthesis in aqueous route and the washing steps, the nanoparticles bear positive surface charges due to adsorption of protons in acidic media, in that case a dilute  $\text{HNO}_3$  solution at pH between 1.2 and 1.7. Therefore the ferrofluid remains in a monophasic state under the application of a magnetic field of arbitrary value. On the microscopic scale, those crystals exhibit a Log-Normal distribution of diameters of parameters  $d_0=7\text{ nm}$  and  $\sigma=0.38$ , as measured by Vibrating Sample Magnetometry (VSM).<sup>2</sup> Maghemite nanoparticles with such a broad size-dispersity can be treated with a size-sorting procedure based on fractionated phase-separation.<sup>3</sup> More precisely, the addition of an excess of  $\text{HNO}_3$  not only lowers the pH but also raises the ionic strength, thereby screening the electrostatic repulsions between the nanoparticles. Above a threshold electrolyte concentration, a liquid-liquid phase separation occurs between a concentrated "liquid-like" phase

and a dilute “gas-like” phase. After magnetic sedimentation on a strong magnet to accelerate demixtion, a concentrated phase (denoted C1) could be readily separated from the supernatant (denoted S1). Then the two fractions were washed by acetone to decrease the ionic strength and redispersed in water. Magnetometry was again used to measure their size distributions, modelled by a Log-normal law with  $d_0$  as median diameter and  $\sigma$  as standard width of the logarithms of diameters:  $d_0=8.8$  nm ( $\sigma=0.36$ ) for C1 and  $d_0=6.6$  nm ( $\sigma=0.31$ ) for S1. The enrichment of the “liquid-like” phase by the larger size tail of the distribution compared to the dilute “gas-like” phase originates from the sensitivity of the inter-nanoparticle potential with the diameters (the larger nanoparticles exhibiting much higher Van der Waals interactions between them). By repeating the phase-separation protocol on both samples C1 and S1, we obtained four new fractions at second level of refined distribution of sizes, and so on after a third and fourth level as indicated on Sketch 1. Among the final products, fractions S1S2S3, S1C2 and C1C2S3S4 were used in this article.

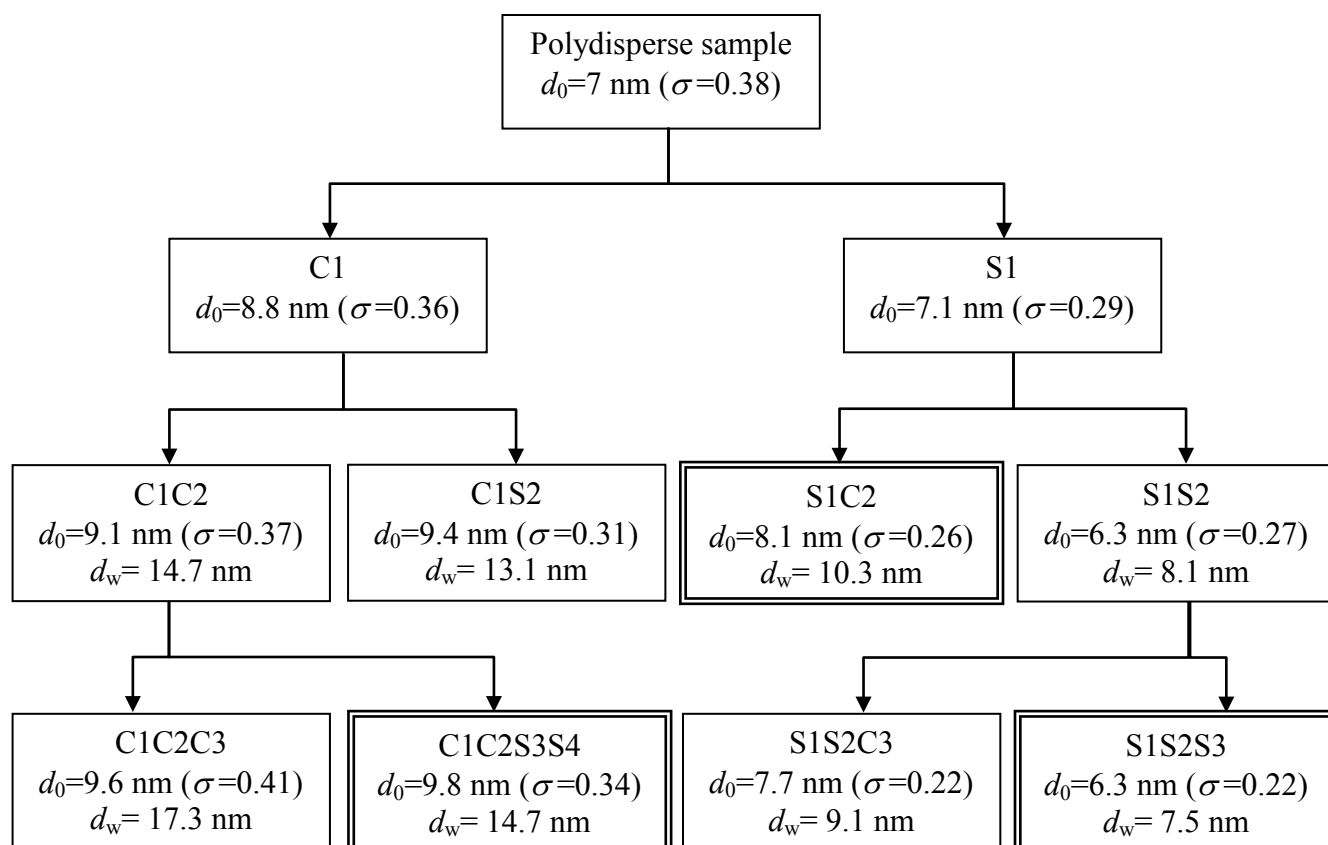


**Figure SI-1:** Chart symbolizing the steps of the size sorting process by successive phase-separation by increase of the ionic strength with excess nitric acid. The fractions of interest are pointed out by a double line frame.

To take into account the residual polydispersity, we estimated a number-average  $d_n$  and a weight-average diameter  $d_w$  for each sample by calculating the 1<sup>st</sup>, 3<sup>rd</sup> and 4<sup>th</sup> order moments of the Log-normal distributions deduced by VSM:  $d_n = \langle d \rangle = d_0 \times \exp(0.5 \sigma^2)$  and  $d_w = \langle d^4 \rangle / \langle d^3 \rangle = d_0 \times \exp(3.5 \sigma^2)$ , which fairly compare to the average diameters  $d_n$  and  $d_w$  from the analysis of electron microscopy pictures while remaining always smaller than the hydrodynamic diameters being measured by dynamic light scattering (Table SI-I).

### SI-3. Characterization of the iron oxide nanoparticles dispersions

The three fractions of interest obtained by the size sorting process (S1S2S3, S1C2 and C1C2S3S4) were characterized before and after the coating with Beycostat NB09 (Table SI-I). DLS measurements as well as TEM pictures showed that the three fractions are well defined in terms of size. Indeed, their mean sizes are distinct for similar values of PDI.

USPIO fraction	$D_H$ of the NPs in aqueous medium (nm) / PDI	$D_H$ of the coated NPs in CH <sub>2</sub> Cl <sub>2</sub> (nm) / PDI	Average diameters by TEM (nm)	Average diameters by VSM (nm)	Saturation magnetization $m_{spe}$ (emu/g)	Blocking temperature $T_B$ (K)	Given name for this work
S1S2S3	7.6 / 0.12	16 / 0.22	$d_n=4.9$ nm, $d_w=6.9$ nm ( $N=600$ )	$d_n=6.5$ nm, $d_w=7.5$ nm	55±1	19.6	6-7 nm
S1C2	18 / 0.07	32 / 0.29	$d_n=8.5$ nm, $d_w=11.6$ nm ( $N=3800$ )	$d_n=8.2$ nm, $d_w=10.0$ nm	62	45.5	8-10 nm
C1C2S3S4	32 / 0.14	23 / 0.15	$d_n=13.8$ nm, $d_w=20$ nm ( $N=1140$ )	$d_n=10.4$ nm, $d_w=14.8$ nm	70±1	114.0	10-15 nm

**Table SI-I:** Different characteristics of the USPIO nanoparticles used in this work: hydrodynamic diameter and polydispersity index determined by DLS before and after surfactant coating, number-average and weight-average diameters measured by fitting the histograms of sizes from TEM images, number-average and weight-average diameters measured by fitting the VSM curves with Langevin formalism using the specific saturation magnetization given by SQUID measurements, and blocking temperatures obtained by zero-field cooled magnetization curves.

Interestingly, the distributions of the particles diameters obtained from the TEM pictures ( $N$  is the counted number of nanoparticles) are well described by Log-normal distributions in fair agreement with those obtained independently by fitting the VSM curves using Langevin formalism.

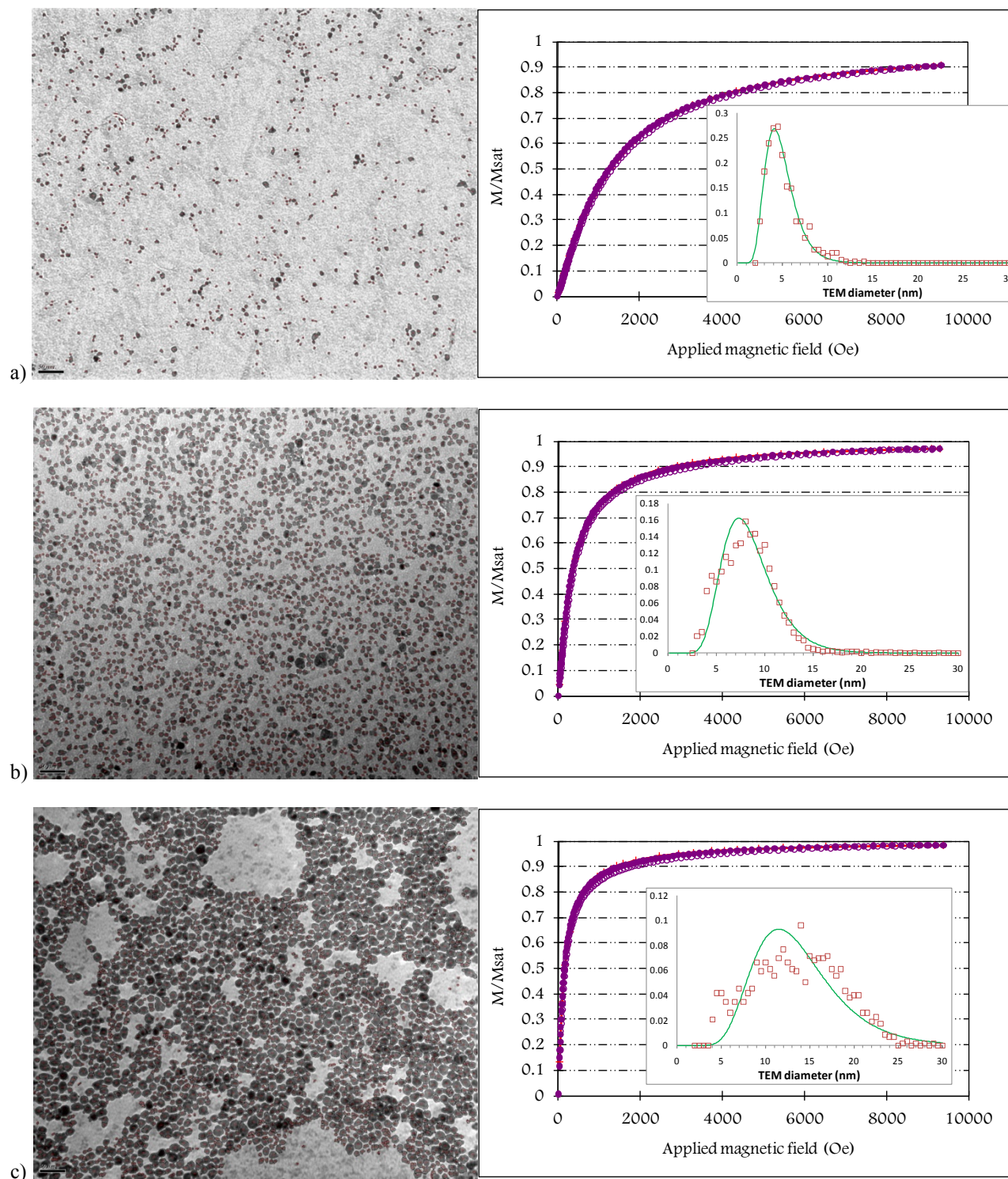


**Figure SI-2:** Analysis of (a) S1S2S3, (b) S1C2 and (c) C1C2S3S4 nanoparticles by TEM (left images) and VSM (right curves). The insets show the experimental distributions of diameters measured with ImageJ on the TEM images (scatter points) and the continuous lines the calculated distributions using the parameters reported in Table S-I. All scale bars' length is 50 nm.

The SAED pattern of the C1C2S3S4 sample, reported in Figure SI-3, show Bragg reflections due to the atomic plans of the nanocrystalline iron oxide  $\gamma\text{-Fe}_2\text{O}_3$  spinel phase (maghemite) according to tabulated data of Miller indexes and inter atomic planes distances.<sup>4</sup>

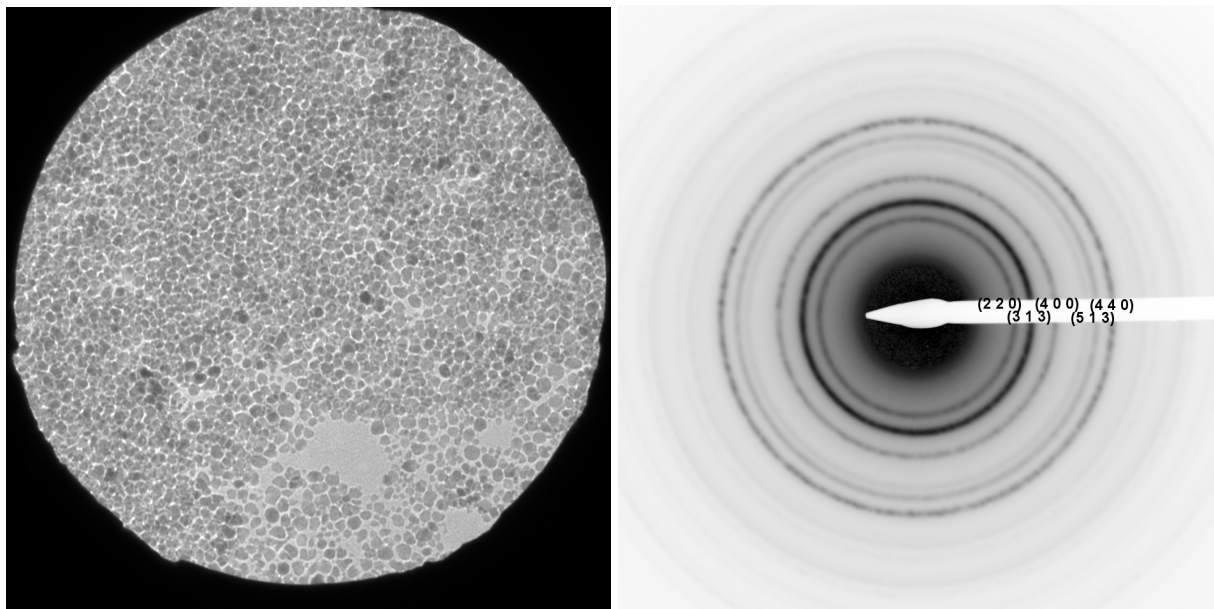


**Figure SI-3:** SAED diffraction pattern of C1C2S3S4 dispersion with rings indexed with the Miller indexes of  $\gamma\text{-Fe}_2\text{O}_3$  corresponding to following experimental (tabulated) inter-planes distances:  $d_{(220)}=2.95(2.95)\text{\AA}$ ,  $d_{(313)}=2.52(2.51)\text{\AA}$ ,  $d_{(440)}=2.08(2.09)\text{\AA}$ ,  $d_{(513)}=1.60(1.60)\text{\AA}$ ,  $d_{(440)}=1.47(1.47)\text{\AA}$ . The dimensions in the Fourier plane were calibrated with the peaks of gold nanocrystals.

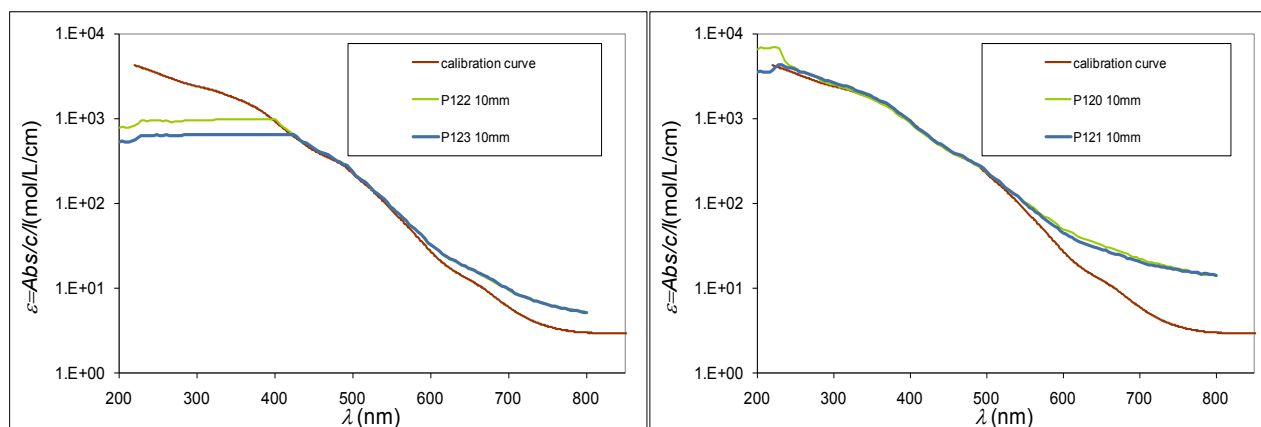


**Figure SI-4:** Examples of iron oxide concentration determination by translation of experimental UV-Vis spectra to fit the calibration curve between 200 and 800 nm.

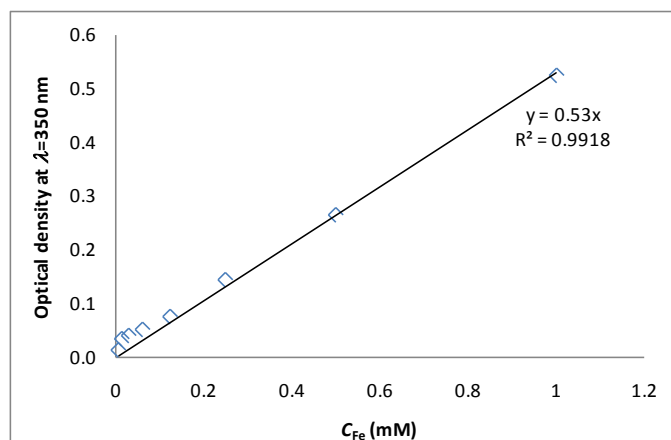


**Figure SI-5:** Calibration curve for the UV-Vis iron titration after dissolving the HNPs and the USPIOs into molecular  $[\text{FeCl}_6]^{3-}$  in  $\text{HCl } 5 \text{ mol}\cdot\text{L}^{-1}$  (light path: 0.2 cm,  $\epsilon_{350\text{nm}}=2800 \text{ mol}^{-1}\cdot\text{L}\cdot\text{cm}^{-1}$ ).

SAMPLE	DISPERSANT	CONCENTRATION OF Fe (mg/L)	CONCENTRATION OF $\gamma\text{-Fe}_2\text{O}_3$ (mg/L)
V6-5	Water	28.5	40.7
V6-10	Water	53.1	75.9
V6-50	Water	325	464.7
V6-50 10X	Water	3500	5000
V6-70	Water	428.9	613.2
V10-5	Water	43.0	61.5
V10-10	Water	77.6	111.0
V10-20	Water	2800	4000
V8-35	Water	330.6	472.7
V8-50	Water	423.9	606.0
M6-5	Water	83.2	119.0
M8-20	Water	731.6	1046
M8-25	Water	876.8	1253.6
M8-30	Water	1038.8	1485.1
M10-20	Water	2300	3300
Endorem <sup>®</sup>	Water	11200 (Supplier)	17300 (TGA)

**Table SI-II:** Concentration of iron or iron oxide in the investigated samples (prior to dilution for the relaxivity measurements).

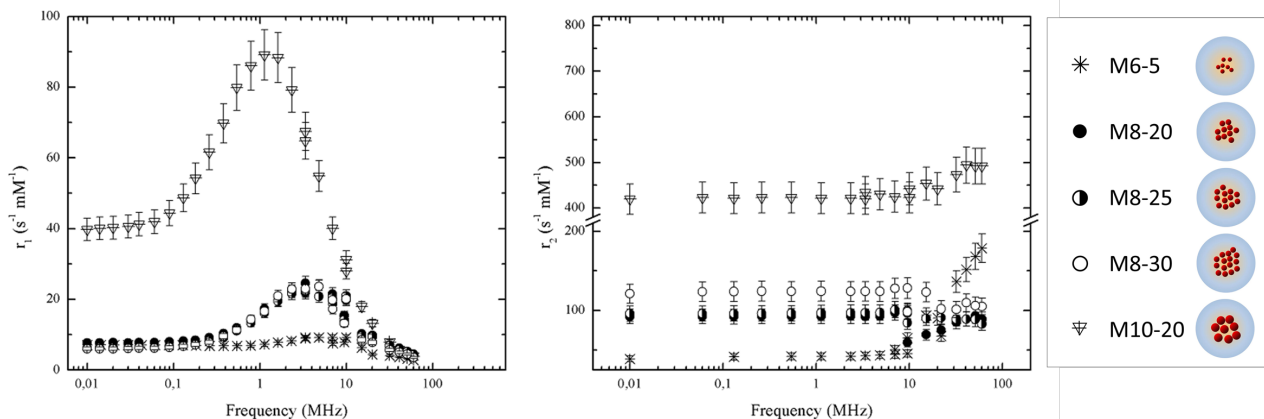


**Figure SI-6:** Longitudinal  $r_1$  (left) and transverse  $r_2$  (right) NMRD profiles for magnetic micelles loaded at different FWRs with the three USPIOs' size (M6-5, M8-20, M8-25, M8-30, and M10-20).

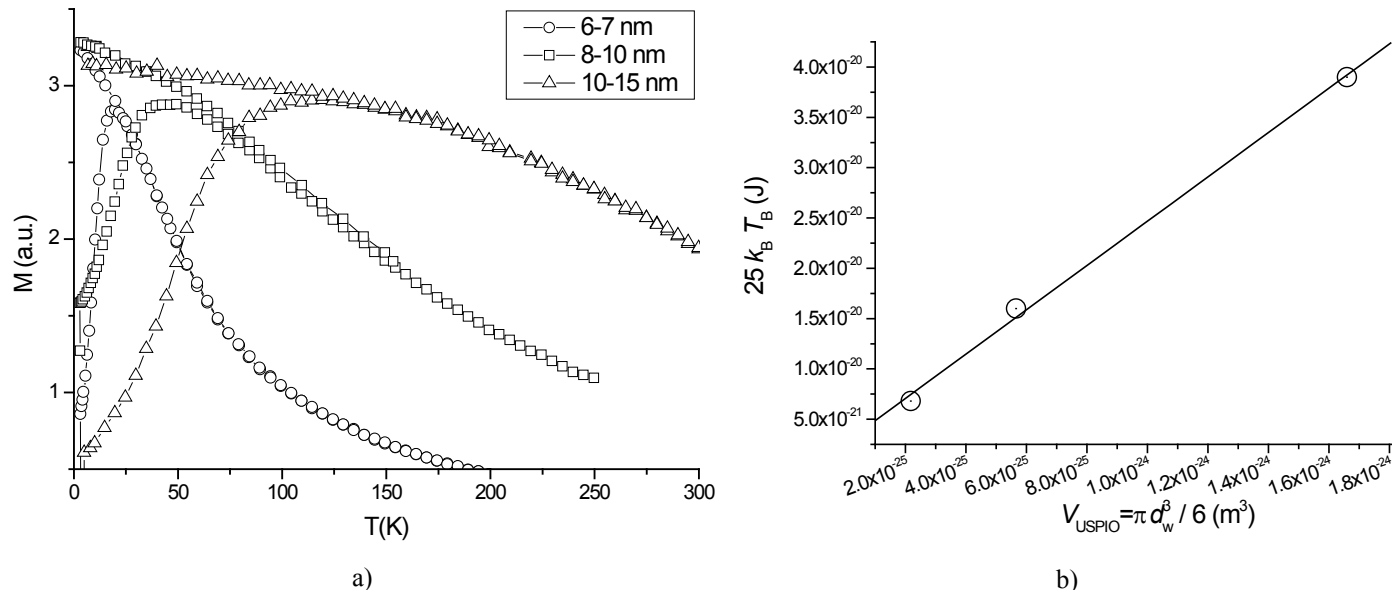


**Figure SI-7:** (a) Zero-Field-Cooled (ZFC) / Field-Cooled (FC) magnetization curves of S1S2S3 (6-7 nm), S1C2 (8-10 nm) and C1C2S3S4 (10-15 nm) nanoparticles. The temperature of the ZFC maxima correspond to the average blocking temperature  $T_B$  associated to the nanoparticle set; (b) Plot of  $25k_B T_B$  vs. weight-average volume of the USPIOs, which slope is equal to the anisotropy constant,  $K_a = 2.4 \times 10^4$  J·m<sup>-3</sup>, a typical value for maghemite  $\gamma$ -Fe<sub>2</sub>O<sub>3</sub> nanoparticles.

## References

- Massart, R., *IEEE Transaction on magnetics* **1981**, 17 (2), 1247
- Chantrell, R. W.; Popplewell, J.; Charles, S. W., Measurements of Particle Size Distribution Parameters in Ferrofluids. *IEEE Transaction on Magnetics* **1978**, MAG-14, 975–977
- Massart, R.; Dubois, E.; Cabuil, V.; Hasmonay, E., *J. Magn. Magn. Mater.* **1995**, 149, 1-5
- R. M. Cornell & U. Schwertmann in "The Iron Oxides" (VCH **1996**)